Estimation of the Noise Contributions from Blank, Transmission and Emission Scans in PET

Søren Holm†, Peter Toft‡, and Mikael Jensen†
† Dept. of Nuclear Medicine, Rigshospitalet, National University Hospital, Copenhagen, Denmark (sholm@pet.rh.dk).
‡Department of Mathematical Modelling, Technical University of Denmark (pto@imm.dtu.dk).

Abstract

This work determines the relative importance of noise from blank (B), transmission (T) and emission (E) scans in PET using a GE Advance scanner on a 20 cm cylinder, a brain phantom, and a torso-like ellipse (18/35 cm) with examples of human scans (brain O-15 water and F-18 FDG, heart FDG). Phantom E scans were acquired in both 2D and 3D modes as decay series with C-11 or F-18 over 3-6 decades of Noise Equivalent Counts (NEC). B and T scans were made using two pin sources (≈500 MBq total) over 64-32768 sec. In humans only a limited subset was available. In homogeneous phantoms normalized variance (var) was estimated from pixel distributions in single images. In other objects, including the human studies, calulations were performed on differences of paired images. In all cases a fit was made to a simple noise model. The cylinder data show expected relations of T to B noise proving the adequacy of B scan times $\leq$ 20 min for most purposes. For the brain phantom, a contour plot is provided for var(E,T). In a typical 3D O-15 water study with 0.5M counts per central slice, a 10 min T-scan adds less than 10% to the total noise level. An example shows how to split a total scan time between E and T scans, in order to minimize the variance.

I. Introduction

PET scans require correction for attenuation in order to be quantitative. Even in brain activation studies where absolute units are often replaced by relative values (i.e., normalized to a mean value), inter-individual comparisons still assume that values across an image reflect the local tracer concentration. Corrections can be applied, e.g., by assuming uniform values of attenuation within geometrically defined boundaries or in segmented areas of the image, but a more accurate description of the attenuation requires measurement by a transmission scan. Unfortunately this also adds noise to the image and adds to the total procedure time. In some cases, mainly in body scanning, the increase in noise is immediately noticed and may even be so high that quantification must be sacrificed in order to provide a reasonable visual impression. However, in other situations, effects that are invisible for the human observer might still be of importance when examining the subtle differences of brain activation by statistical methods. The purpose of this work is to establish guidelines for the relative importance of the noise contributions from blank, transmission, and emission scans in typical imaging situations. Although much information can be deduced theoretically from existing knowledge of reconstruction algorithms [1, 2, 3] we have here applied an experimental approach. The limitations in generality caused by the obvious difficulty of varying all of the many possible parameters of acquisition and reconstruction are outweighed by the advantage of the close reproduction of actual scan setups, including some human studies. The following Section describes the model used for fitting to the observed data. It should not be considered as a rigorous derivation; it merely lists the different structures of the datasets included in the study comprising homogeneous as well as inhomogeneous objects.

II. Theory

Due to the the linearity of the reconstruction process the PET images (volumes) x_i, can be described as a weighted sum of the sinogram values s_j, with weight factors ϕ_{ij} corresponding to the actual (linear) reconstruction algorithm

$$x_i = \sum_j \phi_{ij} s_j \tag{1}$$

where the actual image pixel (voxel) is denoted by i, and j denotes the pixel position in the sinogram. In order to compensate for attenuation the sinogram used for reconstruction is calculated from an emission sinogram e_j, a transmission sinogram t_j, and a blank scan b_j. The calculation basically amounts to:

$$s_j = \frac{e_j b_j}{t_j} \tag{2}$$

although usually qualified by a filtering of the factor $\frac{b_j}{t_j}$.

All three types of sinograms in principle inherit their statistical properties from the Poisson statistics of the radioactive decay. A number of corrections that are performed before the stage of reconstruction described here,

however, adds to the raw counts' noise. The overall effect of correction for randoms and scatter can be described as a decrease in effective counts [4, 3], the resulting figure being widely known as Noise Equivalent Counts (NEC). A practical formulation used in this work is:

$$\mathrm{NEC} = \mathcal{T}\frac{(1-\mathrm{SF})^2}{1+2f\frac{\mathcal{R}}{\mathcal{T}}} \tag{3}$$

where $\mathcal{T}$ is true counts (including scatter), $\mathcal{R}$ is random counts from the full field-of-view, f is the fraction of the sinogram covered by the object under investigation, and SF is the scatter fraction. In all applications of NEC in this study, the value of SF has been set to zero.

While NEC as a global measure may be adequate for the noise description in the case of homogeneous phantoms extending the full axial field-of-view (AFOV), objects of limited extension may be better characterized by a value per slice. In the following, all NEC values quoted correspond to a single slice.

A. *One Emission and One Transmission Scan*

In the simplest case where the image noise is estimated from a single image set, using a Taylor expansion and assuming no noise correlation between pixels implies that the pixel noise variance $V\{x_i\}$ can be estimated by

$$\begin{aligned} V\{x_i\} &\simeq \sum_j \phi_{ij}^2 V\left\{\frac{e_j b_j}{t_j}\right\} \\ &\simeq \sum_j \phi_{ij}^2 E^2\{s_j\}\left(\frac{V\{e_j\}}{E^2\{e_j\}} + \frac{V\{b_j\}}{E^2\{b_j\}} + \frac{V\{t_j\}}{E^2\{t_j\}}\right) \end{aligned} \tag{4}$$

Due to the Poisson statistics the variance in the emission sinogram relative to the squared mean value $\frac{V\{e_j\}}{E^2\{e_j\}}$ is inversely proportional to the mean of an infinite amount of experiments $E\{e_j\}$, i.e., inversely proportional to number of counts NEC in the emission sinogram. Similar arguments can be used for the transmission and blank scan terms, hence the total pixel variance normalized with the mean of the image can be modelled by

$$\frac{V\{x_i\}}{E^2\{x_i\}} = \frac{a}{\mathrm{NEC}} + b + \frac{c}{T_t} + \frac{d}{T_b} \tag{5}$$

where T_t is the transmission scan time in seconds, T_b the blank scan time in seconds (for the given geometry and source strength). In the model a base term b is included to accommodate effects in the reconstruction process, not explained by the other terms, e.g., varying sensitivity of the detectors, not properly corrected for by normalization. For fixed values of (either) T_t or T_b the corresponding terms may also be thought of as part of this constant term. The model applies to regions with limited structural variation, hence measuring variance in a heterogeneous object like the brain or the thorax is problematic.

B. *Two Emission Scans*

To overcome the problem with heterogeneous structures the difference between two PET images, corresponding to two equivalent but independent emission scans $e_j^{(1)}$ and $e_j^{(2)}$, can be calculated. Due to Equations 1 and 2 the difference image is given by

$$x_i = \sum_j \phi_{ij}\left(e_j^{(2)} - e_j^{(1)}\right)\frac{b_j}{t_j} \tag{6}$$

Using a Taylor expansion, and using that the two emission scan have the same mean values $E\{e_j\}$ and variance $V\{e_j\}$ implies that

$$x_i \simeq \sum_j \phi_{ij}\left(\left(e_j^{(2)} - E\{e_j\}\right) - \left(e_j^{(1)} - E\{e_j\}\right)\right)\frac{E\{b_j\}}{E\{t_j\}} \tag{7}$$

Thus the variance $V\{x_i\}$ is given by

$$V_{\text{two e-scans}}\{x_i\} \simeq 2\sum_j \phi_{ij}^2 E^2\{s_j\}\frac{V\{e_j\}}{E^2\{e_j\}} \tag{8}$$

Normalized with the squared mean of the heterogeneous structure and using the same definition of constants as in Equation 5 gives that

$$\frac{1}{2}\frac{V_{\text{two e-scans}}\{x_i\}}{E^2\{x_i\}} \simeq \frac{a}{\mathrm{NEC}} \tag{9}$$

Thus only the emission term of the noise variance can be estimated from two emission scan and one transmission scan. Since all structural information is removed by using differences, no constant term (b) can appear.

If instead two transmission scans (and one emission scan) are available, it is easy to show that two times the transmission variance can be estimated (and only that) from a normalized difference image.

C. *Two Emission and Two Transmission Scans*

Using the same Taylor technique with two sets of emission scans and two transmission scans, it can be shown that

$$\frac{1}{2}\frac{V_{\text{two e and t-scans}}\{x_i\}}{E^2\{x_i\}} \simeq \frac{a}{\mathrm{NEC}} + \frac{c}{T_t} \tag{10}$$

This implies that both the emission and transmission term can be estimated in the inhomogenous case if a double set of independent and equivalent emission and transmission scans are measured and reconstructed pairwise. Note that any normalized variance shown in the following has been divided by two if measured from two scans, cf. Equations 5, 9 and 10.

D. *Zeroes in the Transmission Sinogram*

A common problem especially in body scanning is zeros in the transmission sinogram. One option is to replace

the zeros with a small number T_0, so the attenuation correction can be done cf. Equation 2. Although overflow is avoided this may imply that reconstructed images contain strong lines causing a significant change in the noise structure. Let $\mathcal{Z}$ be the set of j, where the measured t_j is zero. Assume that the variance of the blank scan is negligible and further that only the terms with zeros effectively contribute to the noise. In this case

$$\begin{aligned} V\{x_i\} &\simeq \sum_{j\in\mathcal{Z}} \phi_{ij}^2 V\left\{\frac{e_j b_j}{T_0}\right\} \\ &\simeq \sum_{j\in\mathcal{Z}} \phi_{ij}^2 V\{e_j\}\frac{E^2\{b_j\}}{T_0^2} \end{aligned} \tag{11}$$

This indicates that the number of zeros (through the sum) and the variance on the emission scan determines the noise level. Hence the variance normalized with the squared mean is approximately proportional to the number of zeros and inversely proportional to NEC. In the limit where this kind of noise is dominating, however, the reconstructed images consist of many lines and become useless anyway.

E. *Limitations*

Using either of subsections A, B or C to estimate the noise terms, we estimate the noise variance from a chosen ROI and normalize with the squared mean of the ROI. Due to the global features in the reconstruction process the noise tends to have only a very small correlation with the underlying structure and often it is approximately evenly distributed across the ROI's used. This implies that that the normalized noise variance of the ROI depends strongly on the selected ROI, through the squared mean.

III. Methods

Measurements were made on the GE Advance scanner [5, 6, 7] with 3D acquisition and reconstruction capability. Its 9 GByte raw data disk can hold about 180 3D frames (byte mode, separate prompts and delayed), suitable for phantom decay studies. Reconstruction in our configuration (with 10 i860 processors) takes approximately 8 minutes per frame [8]. For blank and transmission scanning, which is always performed in 2D, the scanner applies two pin sources. During the initial experiments the pin source activities were 389 MBq and 134 MBq, respectively. The blank scan sinogram count rate was 0.91 Mcps, corresponding to an average count rate per sinogram element of ≈ 0.23 cps in the center. On later phantom and human studies, blank and transmission scan times have been scaled in accordance with the currently observed blank scan count rates and the values quoted in seconds are therefore directly comparable.

A. *Phantom studies*

Three different water-filled phantoms have been used: the 20 cm standard (NEMA) cylinder, a torso-like ellipse with axes 18 and 35 cm, and an axially symmetrical, elliptical brain phantom (Capintec) with axes 15 and 20 cm.

Using initially the two homogeneous phantoms in accordance with Equation 5, emission scans were made as decay series with F-18 in 2D (total of 22 measurements) and 3D (only the cylinder, and limited to 10 time frames). Transmission scans were made starting from T_t=64 seconds and doubling the time for each step up to 32768 seconds. Blank scans were made from T_b=64 to 4096 seconds and complemented with one 100000 seconds scan.

Reconstructions were made for all relevant combinations of emission and transmission scans using the 2048 seconds blank scan. All emission scans were further reconstructed with a calculated attenuation correction (CAC) using a circular or elliptical contour respectively. For the 2D cylinder case the emission image with highest count was reconstructed with the longest transmission scan and all blank scans. The cylinder was reconstructed in a 128^2 matrix with pixel size 2.0 mm, and a 4 mm Hann filter. For the ellipse, a 128^2 matrix of pixel size 4.0 mm was used with a 8 mm Hann filter. The 3D axial filter (Hann) was also set to its minimum value of 8.5 mm. The attenuation data were preprocessed with a 8 mm Gaussian filter for the cylinder case, and 10 mm for the ellipse. All available corrections were applied, including detector normalization, randoms subtraction, and scatter correction. In all slices of all reconstructed images (order of 25,000 images) the mean and variance was calculated from an ROI extending 70% of the diameter or ellipse axes. In 2D, the data were averaged over 31 (of 35) slices avoiding edge effects but ignoring the minor differences between direct and cross slices. In 3D only the central 15 slices having almost identical noise were included in the average. For each reconstructed dataset the noise was represented by the normalized variance, i.e., variance/mean^2, in subsequent plots and fitting. From the total rates curves a Noise Equivalent Count (NEC) value per slice was calculated for each scan frame. The rate dependent correction between trues and NECs due to randoms did not exceed 15%.

The brain phantom has two separate chambers ('grey' and 'white' matter, respectively). It was filled to resemble the usually quoted ratio of 4:1 between these two substances for flow or metabolism. Two different sets of measurements have been performed. One set (repeated in 2D and 3D) was originally designed to address count rate performance [9, 10]. The phantoms were loaded with C-11 carbonate well above the expected saturation limit of the scanner and pairs of (60:62) seconds scans were performed every 10 minutes for about 5 hours (15 half lives). The maximum number of slice counts observed in this study was limited to 10^6 which would not allow a suf-

ficiently clear distinction between the transmission scan times. One more decay series was therefore prepared in 3D with F-18 measuring for 12 half lives, each split in two frames with a ratio of (0.415:0.585) yielding approximately equal NEC. The C-11 series were reconstructed using an 'infinite' (32768 sec) transmission scan. For the F-18 series, a set of 6 pairs of transmission scans, 64 - 16384 sec, were obtained. Reconstructions were made to provide datasets with independent transmission and emission noise according to Equation 10 by combining the E-T frames as odd-odd, even-even. Reconstruction parameters for the brain phantom were identical to those for the cylinder except that the axial Hann filter was replaced by a Ramp filter. From both the C-11 series and the F-18 series difference images were calculated, and ROI's placed over grey matter (central and peripheral), white matter, and whole brain in the original as well as the difference images for mean and standard deviation calculation respectively.

B. *Human studies*

For one person (case KL) included in a count rate performance and dose optimization study with O-15 [9], the usual 90 second integration time (starting 20 seconds after bolus injection) was supplemented by 2 short frames (20-22 sec). The study comprised of injections with 25-800 MBq in 2D and 50-800 MBq in 3D. Reconstruction and analysis was performed as above, although only with one 12 minutes transmission scan. The number of NECs in the short scans were about 16% of the corresponding 90 seconds frames normally used.

One person (case MN) injected with 240 MBq of FDG had a double set of emission scans (8-512 sec) of the brain starting 2 hours after injection, followed by a double set of transmission scans (64-512 sec) yielding a total of 28 data points in (E,T)-plane. Reconstruction and data analysis was made to match the brain phantom F-18 series.

One patient (case BB) undergoing a dynamic FDG scanning of the heart additionally had a series of 6 transmission scans (0.5 - 20 min). Pairs of emission scans (0.5,1,2,5 min) from different parts of the dynamic study were reconstructed with all the transmission scans, and subsequent data analysis made as described above (Equation 9) in a large body circumferential ROI.

C. *Fitting data*

From the emission data (see subsections in section II.) the parameter a was estimated by linear regression in a log-log diagram of the normalized variance using the longest transmission scan available. Depending on the setup the transmission parameter c (and the base term b) was subsequently estimated by subtracting the estimated emission part of the normalized variance, a/NEC, and again applying linear regression. This approach is very simple and was considered adequate for the purpose. Non-linear data fitting was also tried and found to give similar results.

IV. Results

In this section data and parameters are presented for the previously described experiments and compared to the model. Again it should be noted that any variance shown has been divided by two if measured from paired difference scans so that the results presented are comparable and represent noise in the single images.

Estimated model parameters from the Cylinder phantom in 2D and 3D modes, the Elliptical Body phantom in 2D, the Brain Phantom, and Case MN, are given in Table 1. This table give parameters valid for any practically used value of NEC and T_t.

Table 1 Estimated model constants.

Case	Mode	a [k counts]	b [ ]	c [sec]
Cylinder	2D	47.7	0.00188	6.40
Cylinder	3D	27.0	0.00035	1.64
Ellipse	2D	24.6	0.00167	8.85
Brain Ph.	3D	16.7		1.01
Case MN	3D	18.5		1.59

In Figure 1 the measured normalized variance in the Cylinder (2D) case is shown. It can be seen that the transmission scans will effectively start to add to the variance if NEC is larger than approximately 10^5 counts per slice and that they - for transmission scan lengths normally encountered - are dominating at 10^7. Note also, that the emission noise model as judged from the linearity in the log-log plot remains valid down to the level where the noise exceeds the mean by an order of magnitude, i.e., beyond any practical application of the images as such.

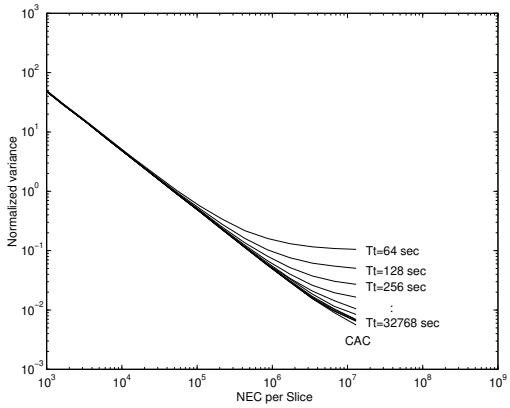

Figure 1 Normalized variance from 2D PET scan of the 20 cm Cylinder phantom as a function of NEC per slice and duration of transmission scan T_t. CAC means calculated attenuation correction.

In the Cylinder (2D) case the blank scan parameter d has also been estimated from reconstructed images corresponding to varying blank scan length T_b, and the estimated value is $d = 0.96$. By comparison with the parameter c from Table 1 the transmission scan in the cylinder case (2D) is seen to contribute approximately 6.7 times more to the variance than a blank scan with the same duration, in accordance with the average attenuation of the central

region of a 20 cm waterfilled phantom.

In Figure 2, corresponding to the Brain phantom scanned in 3D, a contour plot shows the normalized variance as a function of NEC and transmission length T_t. Shading is used to indicate the actual variance, which can be seen from the rightmost grey scale bar. Contours show approximate equidistant level of noise. Furthermore two lines are inserted to show where the transmission term equals 10% and 100% respectively of the emission term.

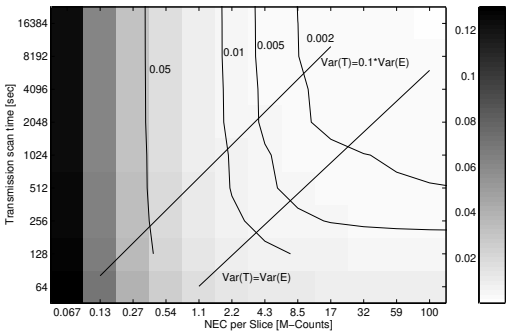

Figure 2 Normalized variance of Brain phantom (3D) as a function of NEC per slice and duration of transmission scan T_t. Contours show iso-noise curves with levels indicated. Lines show where the ratio of transmission to emission noise terms is unity and 10% respectively.

In the Brain phantom (3D) case and in case MN two emission and two transmission scans were measured, thus both emission and transmission parameters have been estimated. The parameters are listed in Table 1. Despite the approximations made for deriving the models Figures 3 and 4 demonstrate an excellent match between the measured data and the model for many decades of NEC. Note that the very low noise level reached in Figures 3 and 5, compared to Figure 1, is due to the use of difference images made from paired emission and transmission scans, which eliminates the b-term.

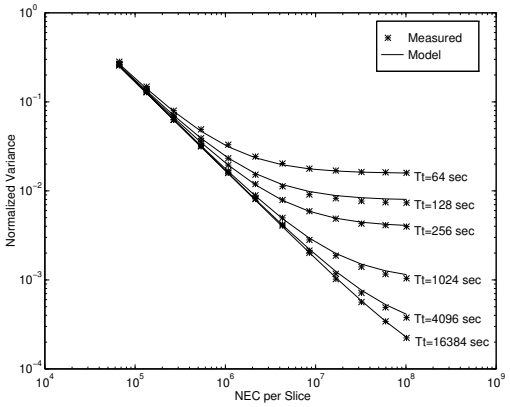

Figure 3 Normalized variance of Brain phantom (3D) as a function of NEC per slice and duration of transmission scan T_t. Stars show the measured data and lines the fitted model.

Figure 5 illustrates how well the emission data measured on human brains agree with the phantom studies. The Figure shows case KL (2D/3D), case MN (2D/3D), and the Brain Phantom (2D/3D). In all cases data corresponding to only one transmission scan are shown.

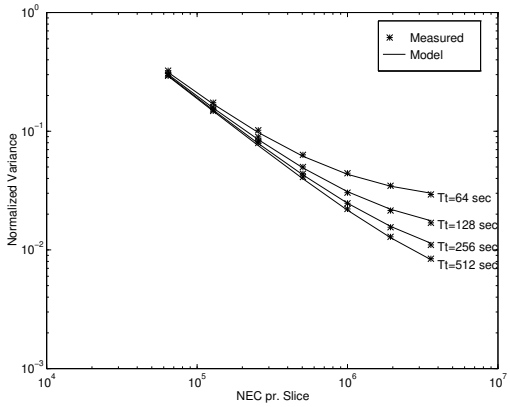

Figure 4 Normalized variance of case MN (3D) as a function of NEC per slice and duration of transmission scan T_t. Stars show the measured data and lines the fitted model.

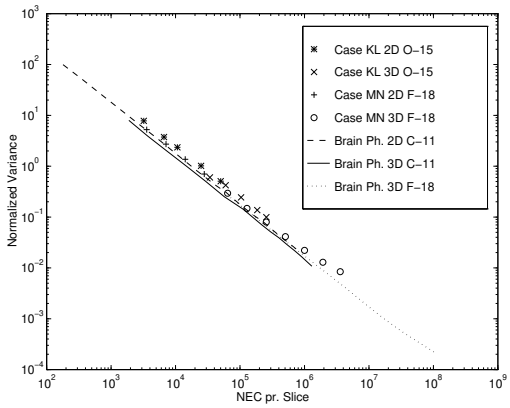

Figure 5 Normalized variance of Case KL (2D/3D), case MN (2D/3D), and Brain phantom (2D/3D) as a function of NEC per slice.

Table 2 shows noise estimates obtained from different ROIs. The emission parameter a and the transmission parameter c have been estimated for the Brain Phantom (3D) in four different ROIs. The Head ROI is an ellipse just surrounding the activity of the brain, WM is a small region within white matter, GM_p and GM_c are two small grey matter regions, peripheral and central, respectively. The averages of the measured regions are normalized to the average of WM. Note the approximately constant ratio between a and c, indicating the major influence of the average on the coefficients.

Table 2 Brain phantom data (3D) with different ROIs.

ROI	a [k counts]	c [sec]	Average
Head	17	1.0	2.07
WM	72	3.7	1.00
GM_p	4.4	0.24	3.98
GM_c	7.2	0.49	4.05

Finally Figure 6 shows data from body measurements. The 2D Elliptical Body phantom follows the previous noise model, but in case BB (large patient with arms in FOV, only a single set of transmission scans) the noise curves for the 1 and 2 minutes transmission scans are shifted

upwards. Inspection of the reconstructed images reveals large number of lines, due to (clusters of) zeros in the transmission scan (cf. Equation 11).

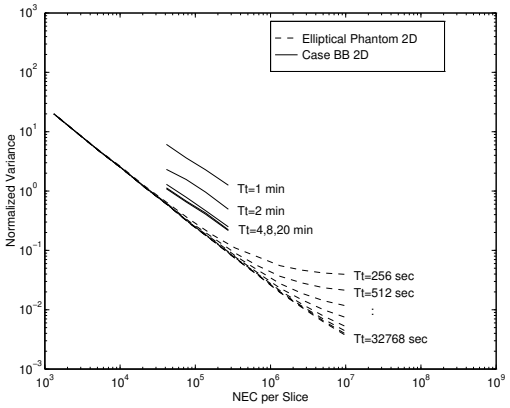

Figure 6 Normalized variance of body studies case BB (2D) and Elliptical phantom (2D) as a function of NEC per slice. Note that case BB (1,2 and 4 min) shows a different noise behavior.

V. Optimization

One application of the estimated noise parameters is optimization of the patient time used in the scanner, [3]. Assume that the total time available for the examination of a patient is T seconds and that the transmission scan and the emission scan are distinct. The duration of the two scans are T_t and T_e respectively, and $T = T_t + T_e$. For simplicity assume that the rate of Noise Equivalent counts is constant and equals R_{NEC}. This implies that the sum of the emisssion and transmission term are given by

$$\frac{V}{E^2} = \frac{a}{R_{\mathrm{NEC}}(T - T_t)} + \frac{c}{T_t} \tag{12}$$

Thus, with respect to the total noise level, the optimum duration of the transmission scan is given by

$$T_t = \frac{T}{1 + \sqrt{\frac{a}{c\ R_{\mathrm{NEC}}}}} \tag{13}$$

Figure 7 shows the normalized variance of the individual noise terms and their sum as a function of transmission scan time T_t. The Figure corresponds to the parameters found in Table 1 for the Brain Phantom (3D) and the sum of the transmission scan time and emission scan time is arbitrarily set to 1800 sec. In Figure 7 it is assumed that $R_{\mathrm{NEC}} = 1000$ counts per slice per sec, which gives an optimized normalized variance of 0.014 when $T_t = 354$ sec. Assuming $R_{\mathrm{NEC}} = 10000$ counts per slice per sec implies that the optimum is found at $T_t = 786$ sec and the normalized variance is 0.0029.

VI. Discussion

The general noise properties of reconstructive tomography are well described in the literature [1, 2]. Previous descriptions of the Advance scanner also include count rate dependence in phantoms and humans [6, 9, 10] but the

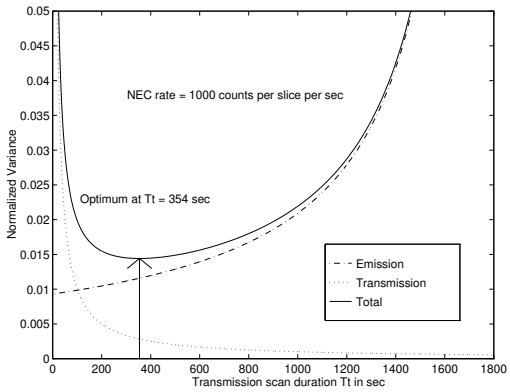

Figure 7 The transmission and emission noise terms and their sum as a function of the transmission scan duration, when the total (patient) scan time is 1800 sec. Parameters correspond to the Brain Phantom (3D). The rate of Noise Equivalent counts is 1000 counts per slice per sec.

noise characterization so far [11] focused on the emission noise. A theoretical derivation [3] using data from the GE 2048 scanner formed part of the basis for the design of the Advance scanner's 2-pin source transmission scanning system. In the present paper we have measured the relative importance of the noise contributions from blank, transmission, and emission scans for a range of imaging situations encountered. Transmission scan values are presented as scan durations in seconds for a given, specified set of sources. Optimal conditions with 2 sources of maximal strength (400 MBq) would almost double the transmission count rate. Given the current expensive Germanium-68 pin sources, the presented configuration represents a likely mean value over source life time. Results can be scaled according to the observed blank scan count rate, to accomodate for differences in number or activity of pin sources and their rotation radius.

An excellent fit to the empirical variance has been found both in 2D and 3D studies. The numerical values of the measure chosen for the noise examination is strongly dependent on reconstruction parameters, in part because of the neighbor pixel correlation disregarded in the theory section. Most parameters, however, will affect the emission and transmission contributions in the same way (through ϕ_{ij} only), and therefore the model and its output is considered adequate for the purpose of identifying areas in the E-T plane where one source is dominating. The analysis largely ignores the fact that the tomographic noise is non-stationary with higher values found towards the center as examplified by the differently located ROIs in the brain phantom, but also in this respect is the ratio between the emission and the transmission term approximately constant.

From the estimated value of $d = 0.96$ it is seen that the blank scan contribution to the noise as expected is only a small fraction of the transmission noise for same duration, the ratio being well explained by the average attenuation of the (central part of) the 20 cm Cylinder phantom. For all practical purposes, therefore, the application of a 20 minutes blank scan will ensure that the blank scan contri-

bution is negligible since the cases where a longer transmission scan might be applied are those with a higher attenuation.

A typical 3D brain activation study with O-15 water in our setup will contain 0.5 Mcounts/central slice, (Figure 5,[9]). With a 10 minute transmission scan, the transmission variance calculated from the phantom data in Table 1 is 0.00167 compared to the emission contribution of 0.0334, i.e., the transmission adds (only) 5% to the final result. If difference images are made, the effect becomes even smaller. For the case MN the corresponding figures would be 0.00265 (transmission), 0.037 (emission) and 7%, respectively. This higher value is due to the lack of a skull for the Brain phantom.

A 10 minute, 2D FDG brain scan typically would also have 0.5-1 M counts yielding the same 5-10% ratio, while acquiring the same data in 3D would make the two contributions almost equal and therefore call for a more detailed analysis of timing. It should be noted that in this imaging condition no attribute has been made to the small additional noise from the emission correction of the transmission scan which is necessary if the transmission is performed with activity present.

Figure 6 suggests that within the emission count range of a typical dynamic heart FDG scan, the emission noise contribution (when using a 20 minute transmission scan) is dominating. Data are, however, currently not available that can demonstrate the region in which the transmission noise curves split up. It should be emphasized that the observed shifts of the curves with short transmission time are due to line-artifacts caused by (clusters of) zeros in the transmission sinogram. This deteriorating effect is usually more important and calls for an improved methods of attenuation correction, e.g., by using image segmentation as described in [12].

VII. Conclusion

The measured image noise variance from a GE Advance PET scanner has been modelled as a sum of terms corresponding to the noise in the emission scan, the transmission scan, and the blank scan. The weight parameters in this simple model have been determined from a large number of experiments for the 20 cm standard (NEMA) cylinder (2D and 3D), a torso-like ellipse with axes 18 and 35 cm (2D), and an axially symmetrical, elliptical brain phantom (Capintec) with axes 15 and 20 cm (3D). Furthermore, noise model parameters have been found from some human studies. For brain studies there is an excellent agreement between model and observation, and between phantoms and human studies. The estimated parameters have been used to optimize the durations of the emission and transmission scan under the constraint that their sum is constant. For studies of the heart or other body regions the model is still generally valid, but the parameters not as well documented, and the transmission noise is often dominated by line artifacts.

References

[1] A. E. Todd-Pokropek and P. H. Jarrit. The noise characteristics of SPECT systems. In P. J. Ell and B. L. Holman, editor, *Computed Emission Tomography*, pages 361–389. Oxford University Press, Oxford, 1982.

[2] N. M. Alpert et al. Estimation of the Local Statistical Noise in Emission Computed Tomography. *IEEE Trans. Med. Imag.*, MI-1(2):142–146, 1982.

[3] C. W. Stearns and D. Wack. A Noise Equivalent Counts Approach to Transmission Imaging and Source Design. *IEEE Trans. Med. Imag.*, MI-12(2):287–292, June 1993.

[4] S. C. Strother et al. Measuring PET Scanner Sensitivity: Relating Count Rates to Image Signal-to-Noise Ratios Using Noise Equivalent Counts. *IEEE Trans. Nucl. Sci.*, NS-37(2):783–788, April 1990.

[5] T. R. DeGrado et al. Performance Characteristics of a Whole-Body PET Scanner. *J. Nucl. Med.*, 35(8):1398–1406, 1994.

[6] T. K. Lewellen et al. Investigations of the Count Rate Performance of General Electric Advance Positron Emission Tomograph. *IEEE Trans. Nucl. Sci.*, NS-42(4):1051–1057, August 1995.

[7] T. Lewellen et al. Investigations of the Performance of the General Electric Advance Position Emission Tomograph in 3D mode. In *Submitted*, 1995.

[8] P. S. Crandall and C. W. Stearns. A Scalable Multi Processor Implementation of the Reprojection Algorithm for Volumetric PET Imaging. In *Conference Record of the IEEE 1995 Nuclear Symposium and Medical Imaging Conference.*, 1996. In press.

[9] S. Holm et al. 3D PET activation studies with $H_2{}^{15}O$ bolus injection. Count rate performance and dose optimization. In *Quantification of Brain Function using PET*. Academic Press, San Diego, 1996. In press.

[10] S. Holm et al. Count Rate Performance and Dose Optimization for rCBF with O-15 Water Bolus Injection in the New 3D PET. *J. Nucl. Med.*, 36:105P, 1995.

[11] S. Pajavic et al. Noise Properties of 3D PET Images. *J. Nucl. Med.*, 36:105P, 1995.

[12] S. R. Meikle et al. Attenuation Correction Using Count-Limited Transmission Data in Positron Emission Tomography. *J. Nucl. Med.*, 34:143–150, 1993.